Polymers **2015**, *7*, 760-776; doi:10.3390/polym7040760

OPEN ACCESS

polymers

ISSN 2073-4360

www.mdpi.com/journal/polymers

Article

Effect of Artificial Weathering on PLA/Nanocomposite Molecular Weight Distribution

Wendy Margarita Chávez-Montes [1,†], Guillermo González-Sánchez [1,†], Erika Ivonne López-Martínez [1,†], Patricia de Lira-Gómez [2,†], Lourdes Ballinas-Casarrubias [3,†] and Sergio Flores-Gallardo [1,*]

[1] Centro de Investigación en Materiales Avanzados, S.C., Miguel de Cervantes No. 120, C.P. 31136, Complejo Industrial Chihuahua, Chihuahua, Mexico;
E-Mails: wendy.chavez@cimav.edu.mx (W.M.C.-M.);
guillermo.gonzalez@cimav.edu.mx (G.G.-S); erika.lopez@cimav.edu.mx (E.I.L.-M.)

[2] Universidad Autónoma de Zacatecas; Unidad Académica de Ciencias de la Tierra, Calzada de la Universidad 108, Zacatecas, Mexico; E-Mail: padelira@gmail.com

[3] Facultad de Ciencias Químicas, Universidad Autónoma de Chihuahua, Circuito Universitario s/n, Campus Universitario No. 2, C.P. 31125, Chihuahua, Mexico; E-Mail: mballinas@uach.mx

† These authors contributed equally to this work.

* Author to whom correspondence should be addressed; E-Mail: sergio.flores@cimav.edu.mx; Tel.: +52-1614-439-1169; Fax: +52-1614-439-4884.

Academic Editor: João F. Mano

Received: 23 January 2015 / Accepted: 16 April 2015 / Published: 22 April 2015

Abstract: The reduction of polylactide acid (PLA) molecular weight for amorphous and semicrystalline grade nanocomposites with 5 wt% load of organomodified montmorillonite Cloisite30B (C30B) was investigated in periods of up to 360 h under artificial weathering. A correlation between artificial and natural weathering was established. The nanocomposites were prepared by mixing the C30B in PLA matrix using two stages of extrusion followed by injection molding. In addition, we also studied materials without C30B in PLA matrix prepared by a single stage of injection, as well as with two stages of extrusion followed by injection, in order to assess thermal effects. XRD (X-ray diffraction) and TEM (Transmission electron microscope) were used to determine the layer dispersion of the C30B within the PLA. An increase in the interlayer spacing of a sandwich structure corresponding to a partial exfoliation of the C30B was found, leading to the creation of

small particles at nanoscale of one (1.29 nm) to eight (11.76 nm) platelets. Also, GPC (Gel permeation chromatography) was used to evaluate the molecular weight decay of neat PLA and its nanocomposites due to thermal processing and subsequent artificial weathering exposure. From thermal processing, a more significant decrease of polydispersity in amorphous PLA than in semicrystalline PLA counterparts could be observed. First order fitting of molecular weight decay of samples *versus* time of exposure under artificial weathering was found for all materials tested. It was observed that the addition of clay favored PLA degradation in amorphous PLA, in comparison with semicrystalline PLA in both thermal processing and artificial weathering. Moreover, a possible effect of C30B interactions with PLA chains under artificial weathering could be postulated.

Keywords: artificial weathering; natural weathering; PLA/nanocomposite; molecular weight; cloisite30B

1. Introduction

The use of long-lasting petrochemical-based polymers for disposable items has considerably disturbed the ecosystem. Therefore, many attempts have been made to substitute petrochemical-based plastics by ecofriendly products. Recently, biodegradable and biocompatible polymers are of increasing focus due to their environmental advantages and mechanical properties which are comparable with conventional plastics. In addition, they are also produced from renewable sources. The most often used biopolymers are polyesters such as poly(ε-caprolactone) [1], poly-vinyl alcohol [2], poly-glycolic acid [3] and polylactide acid [1,3,4]. Polylactide acid (PLA) is a biopolymer derived from the polymerization of lactic acid by a ring opening of its cyclic dimer, lactide. Lactide acid is the basic building block for the production of PLA, where the repeat unit of polymer chain is lactic acid. It is chemically known as 2-hydroxy-propionic acid with two stereoisomers L(−) and D(+) [5]. The chirality of the stereoisomers L(−), D(+) and its racemic mixture D(+), L(−) substantially dominate the properties of PLA: poly(L-lactide) or poly(D-lactide) with high optical purity is semicrystalline. Poly(D,L-lactide) is amorphous [6]. In recent years, there has been an increased demand in the polymer industry for producing stronger films that have better barrier properties than those already on the market. These films are used for farming and food packaging. Because of its biodegradability and mechanical properties, PLA has been previously studied for its use as a food-contact polymer [7,8]. PLA has mechanical properties similar to PET, but has a processing temperature that is significantly lower than PET (polyethylene terephthalate). It has been found that the addition of exfoliated montmorillonite (MMT) clays as filler in composites changes the thermal and mechanical properties compared to PLA without filler [5,9,10]. The nature of the two immiscible components (PLA and MMT) requires the use of organic modifiers in the silicate sheets, which facilitates the dispersion of the filler, achieving the desired properties. If a small percentage of these organomodified MMT is adequately dispersed within the polymer matrix, it creates a larger interfacial area compared to conventional composites [11]. It was found that the organomodified MMT type CloisiteC30B (C30B) significantly improves the mechanical properties of the PLA nanocomposites [4,12,13]. The combination

of PLA and C30B, at nanoscale, often results in remarkably improved mechanical and thermal properties with respect to pure polymers or conventional composites [9]. Furthermore, the molecular weight of PLA is an important property as a degradation indicator. In order to obtain a PLA with improved mechanical properties and environmental-friendly features, both amorphous and semicrystalline PLA nanocomposites were prepared with an organomodified MMT type C30B as reinforcement. For the development of environmental-friendly PLA, the molecular weight distribution plays an important role in controlling the decomposition of PLA. Therefore, PLA nanocomposites with different molecular weights were obtained under the conditions of accelerated weathering. Although the PLA has been studied for decades, information about their degradation by weathering conditions remains limited. Generally, the degradation of a polymer is inherently influenced by their chemical bonds. The lower reactivity of the polymer chain backbone is slowly attacked by external elements. The molecular weight and stereochemistry are important factors that also affect the degradation of polymers. Weathering as a main source of plastic's damage deals with impacts of solar radiation (UV), temperature, and moisture. In natural weathering—with the sun as a radiation source—all impact factors are close to practice, supposing sufficient relevance of the chosen exposure time and site. On the other hand, artificial weathering aims for better reproducibility of natural conditions by using constant or cyclic exposure conditions. Previous studies of PLA nanocomposites indicate that chain scission was the most prominent phenomenon in natural weathering [14]. Zaidi, L. *et al.* (2010) [15] found that the weathering effect on the morphology of exposed samples observed by SEM (Scanning electron microscope) revealed fractured surfaces exhibiting many voids and cracks. These defects were much more pronounced for the PLA nanocomposites. The aim of this work was to study the effect of artificial weathering on the molecular weight decay on two grades of PLA (amorphous and semicrystalline) and its nanocomposites with 5 wt% load of organomodified MMT type C30B. This effect was assessed after considering molecular weight decrease due to thermal degradation inherent to processing for both better C30B dispersion in polymer and film production. Also, it was possible to establish a correlation between natural and artificial weathering.

2. Experimental Section

2.1. Materials

PLA 4060D (amorphous) and PLA 2002D (semi-crystalline) Ingeo Biopolymer, in the form of pellets were supplied by NatureWorks LLC. (Blair, NE, USA). PLA was stored in a dry, cool, and dark place before processing. Molecular weight distribution was determined by GPC. PLA-A (amorphous) and PLA-S (semicrystalline) Number average molecular weight (M_n) was 81.4 and 135.9 kg·mol^{-1} respectively. An organomodified MMT type Cloisite30B (C30B) was purchased in Rockwood Additives (Geretsried, Germany) and used as filler. According to the manufacturer, these C30B were obtained by modification of natural MMT with a quaternary ammonium salt. The main characteristics of the C30B used are displayed in Figure 1 in accordance with the data provided by the supplier.

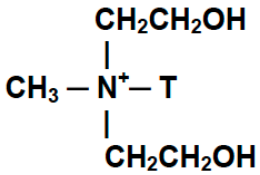

Figure 1. Quaternary ammonium salt used as modification of natural MMT.

Preparation of PLA Nanocomposites and Blanks

Blends of amorphous (PLA-A) and semicrystalline (PLA-S) PLA were performed with 5 wt% load of Cloisite30B (named PLA-A/C30B and PLA-S/C30B, respectively) by Brabender (Duisburg, Germany) DDRV752 corder model extruder. The CloisiteC30B was preconditioned in a drying oven Shell Lab (Cornelius, OR, USA) CE3F at 100 °C during 24 h. First, mixtures were placed in the feed of the extruder, then the experiment was conducted starting at 150 °C in the feed and increased until it reached 180 °C at the die. The materials were prepared at a rotational speed of 20 rpm; the mixtures were ground in a blender to be introduced into another extrusion stage under the same extruder conditions in order to obtain a homogeneous material as a final product. Flexion test tubes of 125.68 mm length, 12.88 mm width and 3.32 mm thick, were prepared by injection molding using a Negri Bossi (Cologno Monzese, Milano, Italy) injection molding machine 55–200 V with mold temperature of 60 °C and die temperature of 220 °C using grounded mixtures coming from the second extruder-stage output. In order to compare the effects of C30B on PLA, two blanks were prepared without the addition of the filler C30B for both amorphous and semicrystalline PLAs (PLA-A/B and PLA-S/B) under the same process to make flexion test tubes of nanocomposites. Additionally, materials without C30B as filler in PLA matrix (PLA-A/P and PLA-S/P) were prepared by single stage injection to observe the effect of PLA degradation only due to injection molding.

2.2. Characterization

PLA pellets were casted into films by taking 5 g of material to undergo melting and compression in a Carver press at a temperature of 200 °C for 20 min and a pressure of 0.5 tons for 1 min, followed by cooling with water flowing inside the plates and by using Teflon sheets between the plates to facilitate removal. Film thickness was measured with a micrometer. The thickness of the films was between 8 and 29 μm. The C30B interlayer spacing (d_{001}) was determined by X-ray diffraction (XRD). Measurements were performed on an X'Pert Pro of PANalytical (Boulder, CO, USA) X-ray diffractometer using Cu Kα. The data was collected over a range of scattering angles (2θ) of 1°–10°. The morphology of the composites was investigated by transmission electron microscopy (TEM). A high resolution JEOL (Tokyo, Japan) JEM2200FS + CS microscope was employed to observe C30B dispersion in PLA matrix. The sample surfaces were cut using a focus ion beam JEOL JEM-9320FIB in thin sections (150–300 nm thickness). The molecular weight distribution and polydispersity index of PLA-A, PLA-S, their blanks, and nanocomposites were determined using a Gel Permeation Chromatograph (GPC) Agilent (Santa Clara, CA, USA) 1200 Infinity Series, using tetrahydrofuran

(THF) HPLC (High Performance Liquid Chromatography) grade as an eluent with an average flow rate of 1.0 $mL \cdot min^{-1}$ at 40 °C using polystyrene standards for calibration. The samples were prepared at a concentration of 1 $mg \cdot mL^{-1}$ in THF.

2.3. Artificial Weathering

The samples were subjected at times of 0, 56, 104, 176, 224, 272, 320 and 360 h on a UV Accelerated Weathering Tester Q-Panel Q-Lab (Westlake, OH, USA) according to cycle 1 of the ASTM (American Society for Testing and Materials) G154: Fluorescent UVA-340 lamp with typical radiation of 0.77 $W \cdot m^{-2} \cdot nm^{-1}$, with maximum peak of intensity in 340 nm, with 8 h of UV exposure period at a black panel temperature of 60 ± 3 °C; followed by a condensation period of 4 h at a black panel temperature of 50 ± 3 °C.

3. Results and Discussion

3.1. Before Accelerated Weathering

3.1.1. XRD

The beam incidence angle 2θ was measured in the range of 0°–10° because the main peaks of the C30B are in this range [16]. Moreover, according to Picard, E. *et al.* (2011) [17], diffraction peaks observed in this range are associated with intercalated clay state within the PLA matrix composites. The XRD patterns of C30B (powder) and PLA-based nanocomposites (as films) are presented in Figure 2. The diffraction pattern of C30B exhibits a sharp peak at 2θ = 4.77°, corresponding to an interlayer spacing (d_{001}) of 1.85 nm. Note that these results agree with those of Paul *et al.* (2005) [18], where the mean of interlayer spacing for the C30B was 1.82 nm corresponding to 2θ = 4.85°. As a reference, natural MMT clay shows a smaller interlayer spacing of 1.2 nm without the organic modification [19]. The organic modification leads to an increase of the interlayer spacing, due to the presence of the modifier between the MMT platelets.

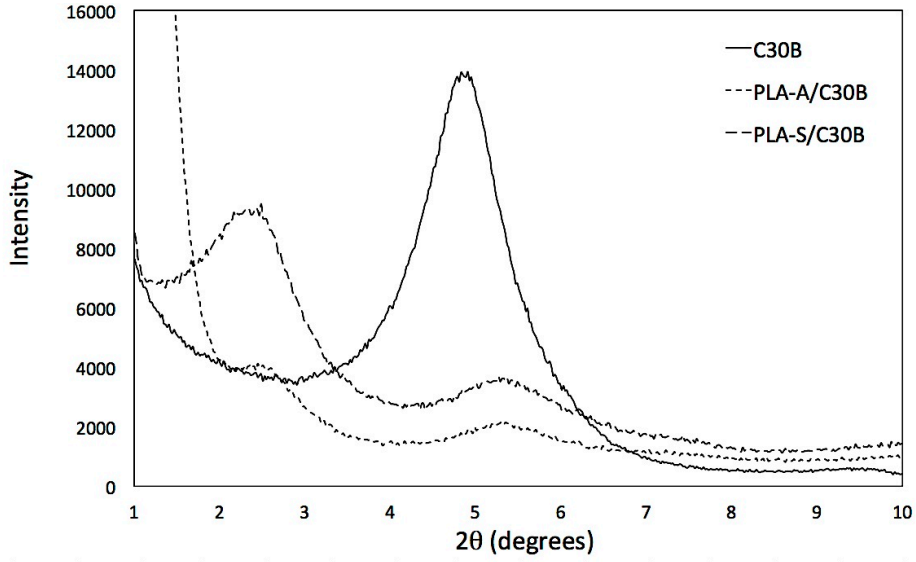

Figure 2. XRD of PLA nanocomposites and organic modified MMT (C30B) used as filler.

For PLA nanocomposites the addition of C30B produced a peak shift of X-ray diffraction angle 2θ to a lower angle (2°–2.5°) compared to the pure C30B (4.77°). This is attributed to the strong interaction and miscibility between PLA and C30B, which originates from the strong hydrogen bonding among carboxyl groups of PLA and hydroxyl groups of C30B. Similar studies on polymer/clay nanocomposites indicate that strong polar-type interactions were favored especially on exfoliated hybrids via polymer intercalation [20–22]. PLA chains were inserted between the C30B galleries increasing its interlayer spacing d_{001} to 3.85 and 4.06 nm in PLA-A/C30B and PLA-S/C30B, respectively. However, a second diffraction peak was observed at a greater angle (5°–5.2°) on both composites. According to Najafi, N. *et al*. (2012) [13], the second peak may be the result of the collapse of the clay galleries in the d_{002} plane due to thermal degradation of the organic component of the clay.

3.1.2. Morphology

TEM analysis can be used to support XRD results by visualizing C30B dispersion at nanoscale. Typical TEM micrographs of PLA composites both amorphous and semicrystalline are shown in Figure 3. Dark lines correspond to the cross section of the clay layers and the gap between the two adjacent lines is the interlayer space. It was observed that clay galleries were broken down due to the applied shear stress during extrusion and injection. Particles, which consist of well-aligned and regularly spaced platelets in the nanometer range, were observed with thickness starting from 1.29 nm (Figure 3a) up to 11.76 nm (Figure 3d), corresponding to a single platelet and eight platelets of clay, respectively. Particles of three and four stacked platelets were also often observed as shown in Figure 3b,c. The combination of polymer and C30B at nanoscale often results in remarkably improved mechanical and thermal properties in comparison to pure polymers or conventional composites [9].

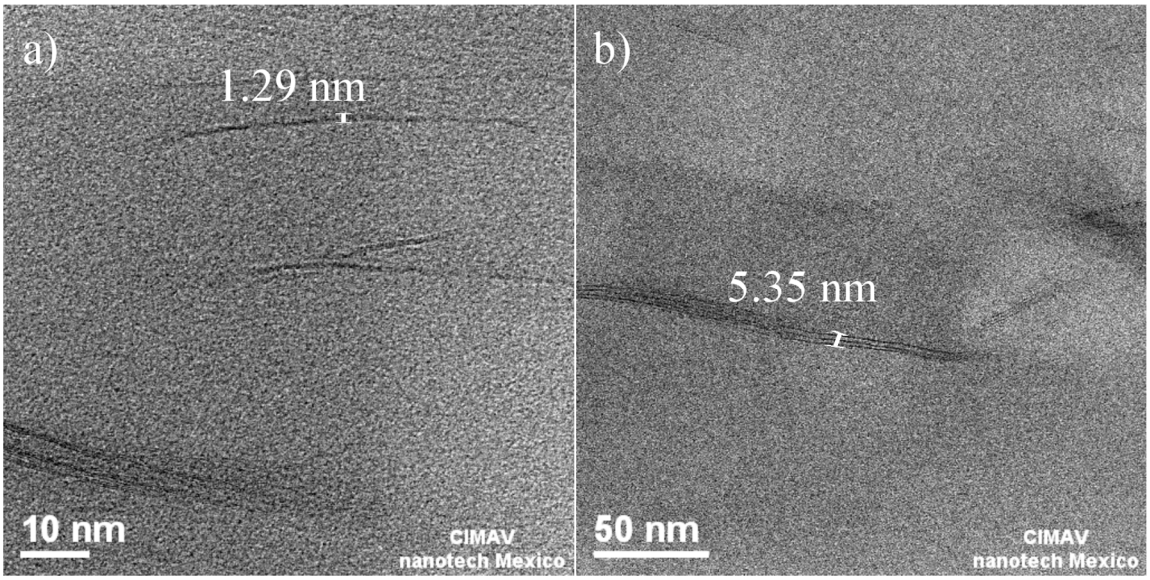

Figure 3. *Cont.*

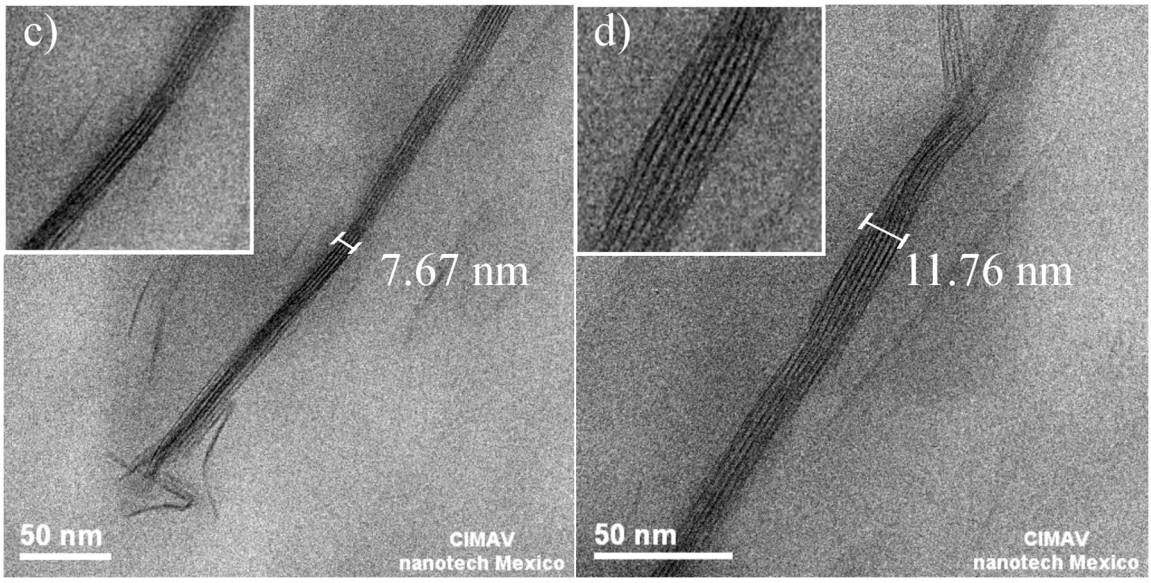

Figure 3. TEM micrographs of (**a**) PLA-A/C30B single platelet; (**b**) PLA-A/C30B three stacked platelets; (**c**) PLA-S/C30B four stacked platelets; (**d**) PLA-S/C30B eight stacked platelets.

3.1.3. Molecular Weight Distribution before Artificial Weathering

It is well known that PLA is susceptible to thermal degradation during the melting process revealing a loss of number average molecular weight (M_n) from 20% to 80% [23]. Thus, it was necessary to elucidate the effect of thermal degradation due blending between PLA and C30B and the molding process of test tubes on Molecular Weight Distribution (MWD). In order to study the degradation effect of C30B into PLA matrix, it was necessary to analyze M_n, Weight Average Molecular Weight (M_w) and polydispersity index (M_w/M_n) to understand their changes during processing. Therefore, GPC analysis was performed on all samples before (Table 1) and after (Table 2) artificial weathering.

Table 1. MWD of samples before artificial weathering.

Sample	M_w (kg·mol^{-1})	M_n (kg·mol^{-1})	M_w/M_n
PLA-A/Neat	270.0	81.4	3.32
PLA-A/P	157.8	57.0	2.77
PLA-A/B	139.0	50.3	2.76
PLA-A/C30B	97.7	44.7	2.19
PLA-S/Neat	329.0	136.0	2.42
PLA-S/P	222.7	77.0	2.90
PLA-S/B	125.0	49.0	2.55
PLA-S/C30B	99.0	43.5	2.27

A reduction on M_n in amorphous PLA was observed from 81.4 kg·mol^{-1} in PLA-A/Neat to 57.0, 50.3 and 44.7 kg·mol^{-1} for PLA-A/P, PLA-A/B and PLA-A/C30B, respectively. PLA-S/Neat with an initial M_n of 135.9 kg·mol^{-1} from the original pellets diminished to molecular weights of 77.0, 49.0 and 43.5 kg·mol^{-1} on PLA-S/P, PLA-S/B and PLA-S/C30B, respectively. This decrease of about 30% and 40% PLA-A/P and PLA-S/P occurred during a single stage of injection molding, while

PLA-A/B and PLA-S/B decrease was about 38% and 64%, respectively, as a consequence of the two extrusion stages and injection molding. It can be observed from Table 1 that semicrystalline PLA without C30B (PLA-S/P and PLA-S/B) showed greater resistance to degradation than amorphous PLA also without C30B (PLA-A/P and PLA-A/B) during processing (extrusion and injection molding). This can be attributed to strong interaction of chains in crystalline regions; thus, more energy is required to break down crystalline chain interactions compared to the energy required to break down intermolecular interactions on amorphous regions. According to Mróz, P. *et al.* (2013), [9] nano-additives introduced to polymers can simultaneously modify their degradation rate and mechanism. Dependent on the chemical structure of additives and possible interactions with polymers, their presence in composites leads to an increase or decrease on their thermal stability. We could observe a M_n decrease of about 45% in PLA-A/C30B and 68% in PLA-S/C30B nanocomposites during processing, which indicates an increase in degradation of nanocomposites in comparison with their blanks. This decrease in M_n and M_w due to processing was considered as the basis for establishing the forward molecular weight decay of PLA under artificial weathering. On the other hand, polydispersity index (M_w/M_n) displayed a relative stability with values between 2.27 and 2.77. This strongly suggests that chain scissions randomly occurred in all the macro-molecules of the PLA under thermooxidative and shear forces from extrusion, and injection molding. Therefore, the molecular weights decay on samples only injection molded can be attributed to shear stress and processing temperature (220 °C at the die). However, samples that were prepared under two stages of extrusion and latter injection molded (PLA-A/B, PLA-A/C30B, PLA-S/B and PLA-P/C30B) showed greater molecular weight decay due to temperature (180 °C at the die) and shear stress during extrusion.

3.2. Molecular Weight Distribution after Artificial Weathering

Figure 4 shows the change in normalized form of MWD obtained by GPC, of PLA pellets from the original material, nanocomposites and blanks after different durations of weathering. Average molar mass values and polydispersity index are listed in Table 2. Chromatographic elution of materials shift to longer retention time as the exposure time to artificial weathering was increased, indicating a reduction in chain size of PLA in the studied materials. In agreement with prior reports, significant molar mass reduction under PLA artificial weathering was observed [3]. The initial M_w on amorphous PLA, that was only injection-molded (PLA-A/P), was reduced from 157.8 to 13.5 kg·mol^{-1} after 360 h under artificial weathering. M_w of semicrystalline PLA only injection molded (PLA-S/P) showed a major decrease from 222.7 kg·mol^{-1} of its initial M_w to 33.7 kg·mol^{-1} after 360 h of exposure to artificial weathering. These results show that PLA-A/P has a major molar mass decrease about 70%, than PLA-S/P about 44% of initial M_w. A similar effect was observed also on the rest of the samples. A resistance to artificial weathering was observed on semicrystalline PLA; this might be due to the fact that the arrangement of chains in crystalline regions were degraded slower than those in the amorphous regions, which indicates that crystalline regions require more energy to lead chain breakage. A similar result was also observed by Tsuji, H. *et al*. (2006) [1], where they showed that the photodegradability of PLA chains in the crystalline region was lower than that in the amorphous regions. The latter report can be compared to artificial weathering where photodegradation is taken as the main source of energy that leads to chain breakage.

Table 2. MWD of degraded samples under artificial weathering.

Sample	Exposure time (h)	M_n (kg·mol^{-1})	M_w (kg·mol^{-1})	M_w/M_n	Sample	Exposure time (h)	M_n (kg·mol^{-1})	M_w (kg·mol^{-1})	M_w/M_n
PLA-A/Neat	-	81.4	270.0	3.32	PLA-S/Neat	-	136.0	329.0	2.42
PLA-A/P	0	57.0	157.8	2.77	PLA-S/P	0	77.0	222.7	2.90
	56	37.5	81.0	2.16		56	44.1	106.0	2.40
	104	39.8	96.0	2.41		104	41.2	80.9	1.97
	176	26.8	59.7	2.22		176	37.5	92.3	2.46
	224	23.5	52.2	2.22		224	22.1	47.4	2.15
	272	21.3	44.7	2.10		272	23.8	51.1	2.14
	320	11.3	26.1	2.31		320	17.7	35.2	1.99
	360	6.73	13.5	2.01		360	16.9	33.7	2.00
PLA-A/B	0	50.3	139.0	2.76	PLA-S/B	0	49.0	125.0	2.55
	56	48.0	150.0	2.40		56	42.9	107.0	2.49
	104	42.1	102.0	2.42		104	34.6	81.1	2.35
	176	26.3	60.5	2.30		176	33.1	74.3	2.25
	224	22.4	50.8	2.27		224	21.6	47.0	2.17
	272	14.7	29.3	1.99		272	21.3	45.1	2.11
	320	11.8	23.6	2.00		320	20.4	43.1	2.11
	360	7.58	15.8	1.99		360	16.4	33.3	2.03
PLA-A/C30B	0	44.7	97.7	2.19	PLA-S/C30B	0	43.5	99.0	2.28
	56	30.9	65.9	2.14		56	38.1	89.2	2.34
	104	23.0	43.2	1.88		104	34.0	74.8	2.20
	176	12.7	25.0	1.97		176	31.9	69.7	2.19
	224	11.5	18.9	1.64		224	17.1	31.0	1.82
	273	9.4	14.2	1.51		273	12.6	21.1	1.68
	320	8.7	12.7	1.45		320	14.7	25.6	1.74
	360	7.8	9.7	1.24		360	11.3	22.8	1.73

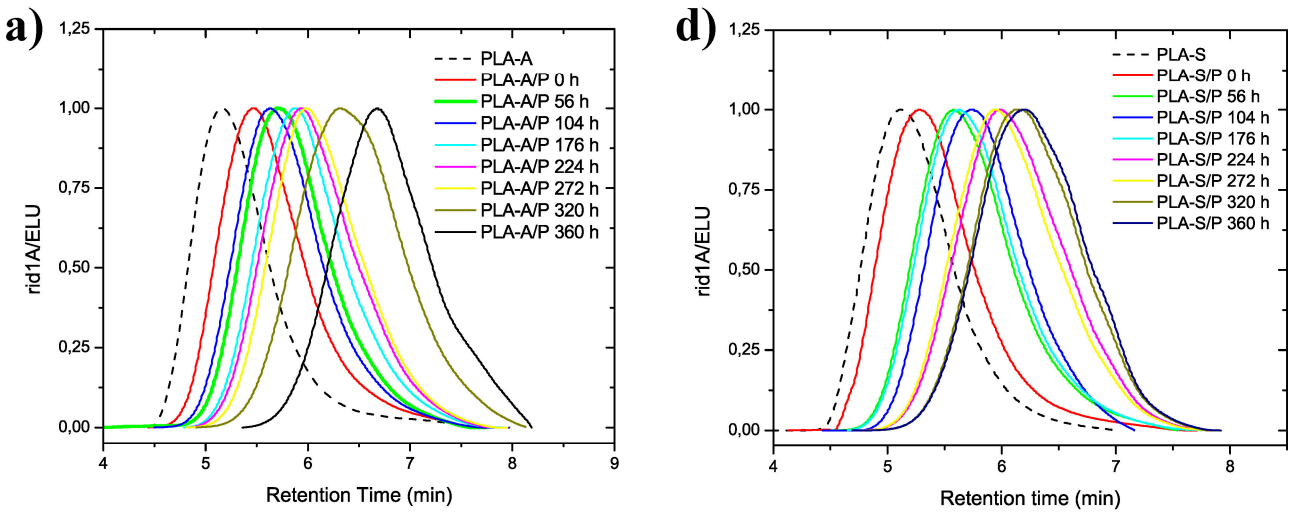

Figure 4. *Cont.*

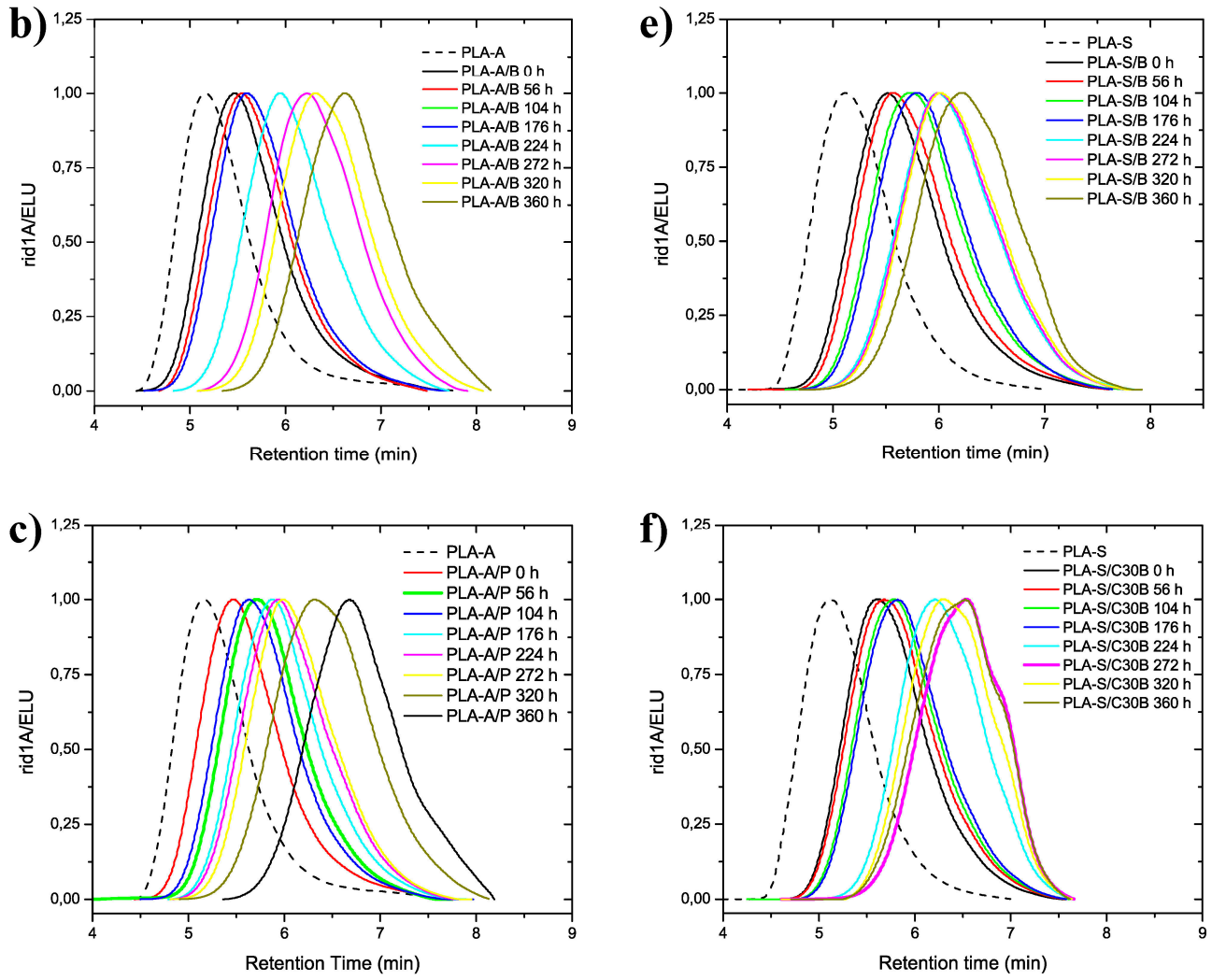

Figure 4. MWD of (**a**) PLA-A/P; (**b**) PLA-A/B; (**c**) PLA-A/C30B; (**d**) PLA-S/P; (**e**) PLA-S/B; (**f**) PLA-S/C30B at different times of exposure to artificial weathering.

Moreover, a systematic molecular decrease with the increase on the exposure time (from 0 to 360 h) of the specimens, subjected to artificial weathering, was observed. Since every material started with a different M_n and M_w, we present the results of M_n and M_w decay as percentages of degradation in order to make them equivalent on each material for a valid comparison. Percentages of M_n and M_w degradation of samples under artificial weathering are shown in Table 3 and Figure 5. A larger decrease in M_w than in M_n is associated with a reduction on polydispersity index on amorphous, semicrystalline, and nanocomposites of PLA, indicating that short chains (small molecular weight) break down easily, while long chains (big molecular weight) require more energy to break down. This effect was more pronounced in nanocomposites than in PLA without C30B. Generally speaking, a major degradation was observed in PLA-A in comparison to PLA-S for all materials. M_n and M_w drop off for the greatest exposure time on PLA-A/P (only injection molded) to 88% and 91%, respectively. Meanwhile, M_n and M_w drop off on PLA-S/P to 78% and 85%. The same decay tendency was observed on PLA blank and nanocomposites, with degradation of 89% in PLA-A/B, and 73% in PLA-S/B both on M_w. Also, degradation of M_w of 90% and 70% was observed in PLA-A/C30B and PLA-S/C30B, respectively.

Table 3. Percentages of M_n and M_w degradation of samples under artificial weathering.

Sample	Exposure time (h)	% M_n Degradation	% M_w Degradation	Sample	Exposure time (h)	% M_n Degradation	% M_w Degradation
PLA-A/P	0	-	-	PLA-S/P	0	-	-
	56	34	49		56	43	53
	104	30	39		104	47	64
	176	53	62		176	51	59
	224	59	67		224	71	79
	272	63	72		272	69	77
	320	80	83		320	77	84
	360	88	91		360	78	85
PLA-A/B	0	-	-	PLA-S/B	0	-	-
	56	5	-8		56	12	15
	104	16	27		104	30	35
	176	48	56		176	33	41
	224	55	63		224	56	63
	272	71	79		272	56	64
	320	77	83		320	58	66
	360	85	89		360	67	73
PLA-A/C30B	0	-	-	PLA-S/C30B	0	-	-
	56	31	33		56	13	10
	104	48	56		104	22	24
	176	72	74		176	27	30
	224	74	81		224	61	69
	273	79	85		273	71	79
	320	80	87		320	66	74
	360	82	90		360	74	77

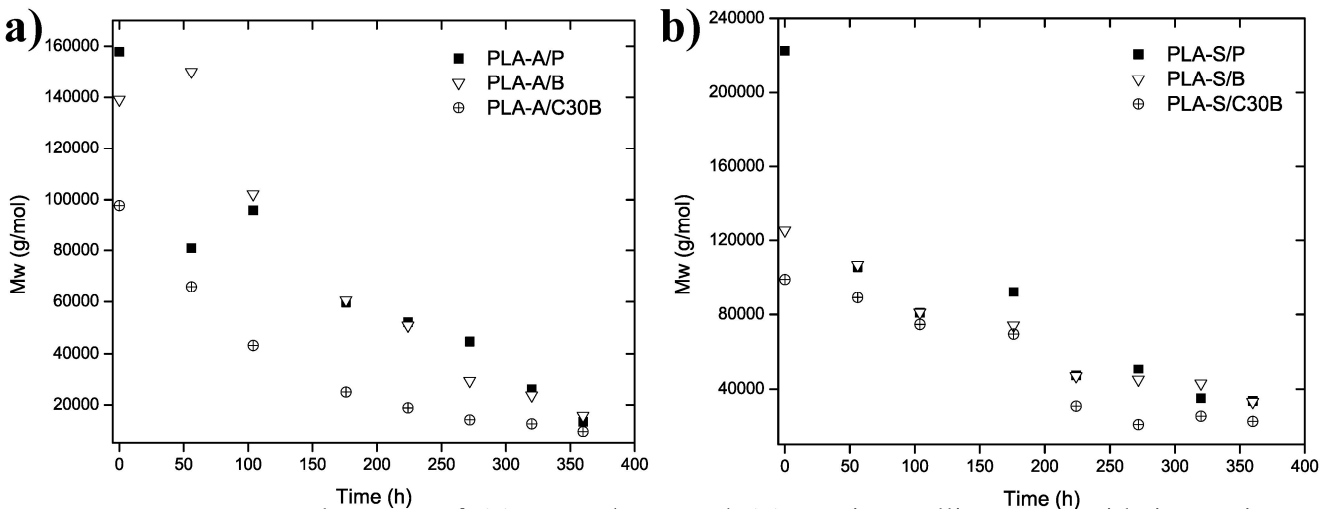

Figure 5. M_w decrease of (**a**) amorphous and (**b**) semicrystalline PLA with increasing exposure time to artificial weathering.

Figure 6 presents the evolution of polydispersity index (M_w/M_n) of amorphous Figure 6a and semicrystalline Figure 6b PLA as the duration of accelerated weathering conditions was increased.

As shown, in all samples of PLA, M_w/M_n decreases during the artificial weathering, and this fact is better known in PLA nanocomposites. The polydispersity index of amorphous PLA nanocomposite (PLA-A/C30B) gradually decreased during 360 h of exposure time, which resulted in the value of M_w/M_n = 1.24. While, the polydispersity index of semicrystalline PLA nanocomposite (PLA-S/C30B) did not show any significant changes at 176 h of exposure. However, this property decreased gradually at 272 h of exposure (M_w/M_n = 1.68). The decrease in polydispersity index of PLA nanocomposites is explained by the combined effect of hydrolysis (condensation period) and photodegradation (UV exposure period) due to accelerated weathering conditions, which are produced by chemical cleavage of the main polymer chain by the reaction with water, initiated by protonation, followed by the addition of water and cleavage of the ester linkage.

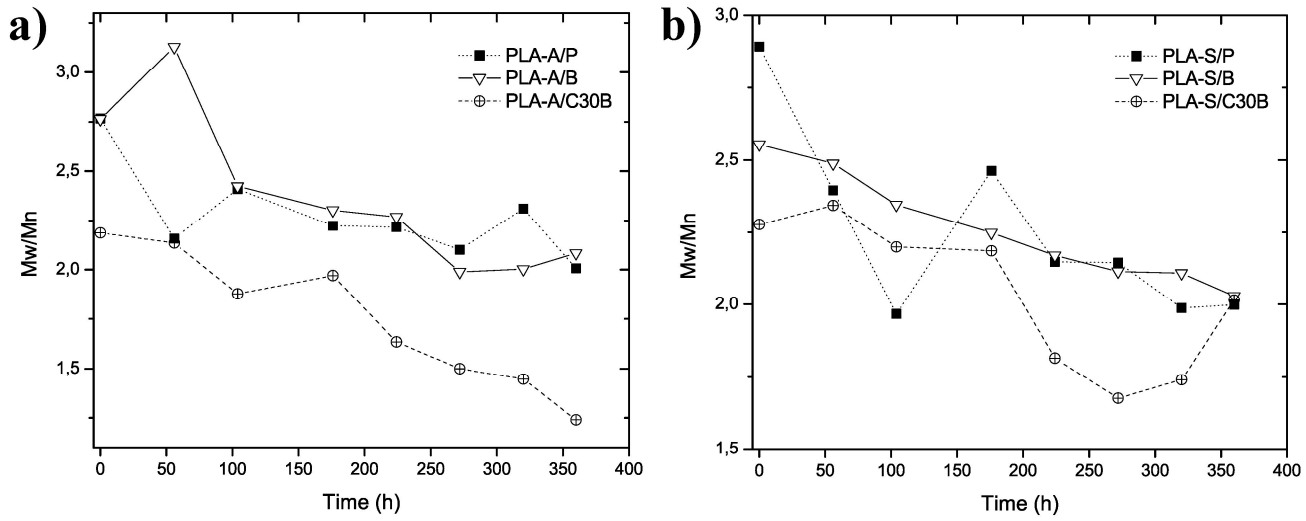

Figure 6. Polydispersity index of (**a**) amorphous and (**b**) semicrystalline PLA as exposure time to artificial weathering was increased.

The lowest M_w range was from 13.5 to 15.8 kg·mol^{-1} for PLA-A samples without addition of C30B and 33.7–33.3 kg·mol^{-1} for PLA-S samples also without addition of C30B at longer exposure time (360 h). Although there have been several studies about the mechanism of photodegradation in the areas of PLA, a definite mechanism has not yet been found [24,25].

4. Number Average Molecular Weight Decay Due to Artificial Weathering

On exponential decay, a quantity is subjected to exponential decay if it decreases at a rate proportional to its current value. In order to predict the PLA M_n when exposed to artificial weathering, it was necessary to establish a relationship between the hours of exposure to artificial weathering regarding the loss of molecular weight. Thus, a first order fitting was established for such relationship. Figure 7 shows the experimental data fitting of the studied materials. Previous studies have described the degradation of PLA as a random chain breaking reaction [1,26], which is associated with a first order decay. In this paper, the fitting first order decay of M_n was studied under the conditions of artificial weathering.

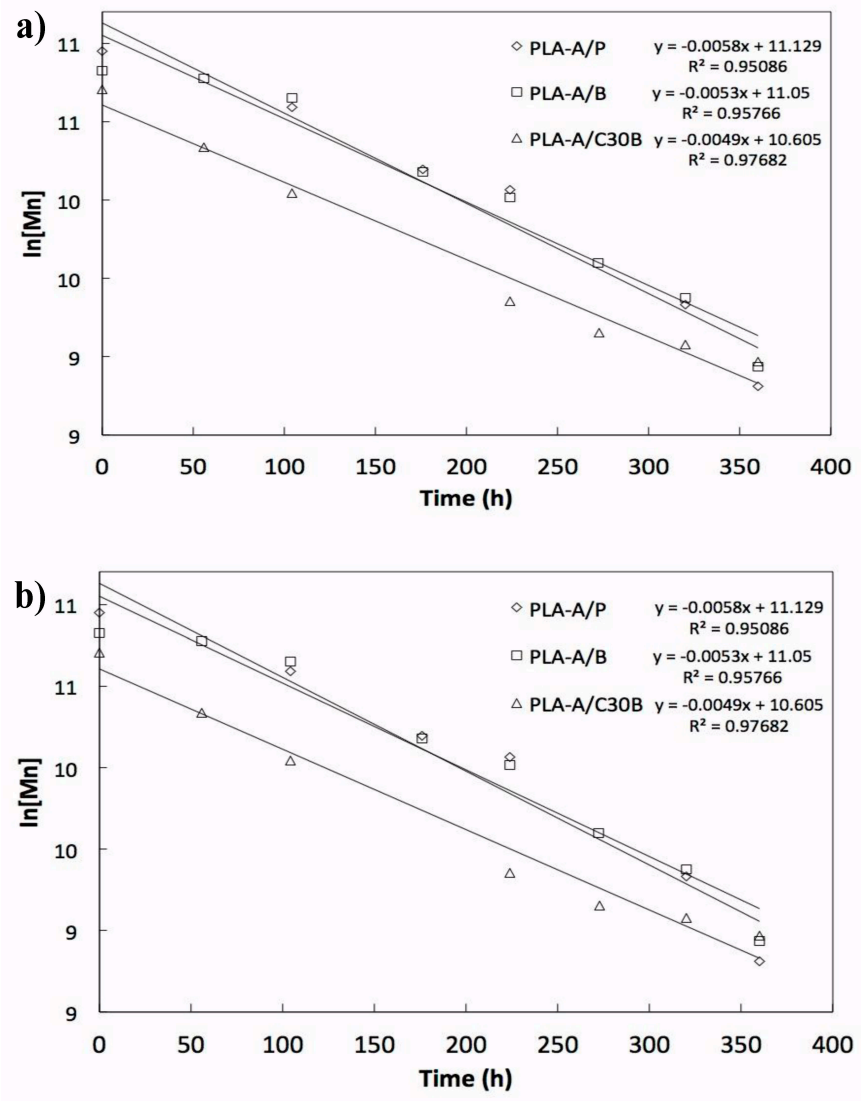

Figure 7. First order decay of (**a**) amorphous and (**b**) semicrystalline PLA molecular weight.

The correlation coefficients (R^2) in model fitting first order decay were 0.8982, 0.9577 and 0.9521 for PLA-A/P, PLA-A/B and PLA-A/C30B, respectively, on amorphous PLA. Moreover, the model fitting first order decay in semicrystalline PLA materials showed a R^2 of 0.9333, 0.955 and 0.9079 for PLA-S/P, PLA-S/B, PLA-S/C30B, respectively. In addition, a rate of reaction for all materials in order to be compared between both types of PLA (amorphous and semicrystalline) was calculated. The constant rate of first order reaction (k) of amorphous PLA materials took values from 0.0049–0.0052 h^{-1}. It can be seen that the values of k in PLA-A are greater than those of PLA-S (0.004 h^{-1}), which reveals slower chain degradation in the crystalline regions compared to the amorphous regions. We also observed that k was greater in nanocomposites than on neat samples. It is clear that C30B has enhanced the degradation process in PLA nanocomposites. This effect can be attributed to the addition of C30B due to the strong interaction and miscibility between PLA and C30B which can be attributed to the strong hydrogen bonding among carboxyl groups of PLA and hydroxyl groups of C30B. Thus, when UV radiation is absorbed by C30B, it promotes radical generation on the organomodified section of C30B. The same effect of the MMT on the degradation process was found on Polyethylene (PE) nanocomposites [27]. According to Kumnayaka, T. *et al.* [27], the MMT acts as

a catalyst of the photo-oxidation reaction. They observed a decrease in the molecular weight of the PE/MMT nanocomposites that was attributed to the occurrence of chain scission reactions during photo-oxidation. In addition, Zaidi, L. *et al.* [15] showed that the photo-oxidation rates of PLA were increased in the presence of C30B. Also, the same effect of the MMT into PLA matrix on the degradation rate was found by Araujo, A. *et al.* [28].

Correlation of Artificial Weathering with Natural Conditions

In this study, the local geographic area was selected according to the ASTM D5272, with desert characteristics similar to that found in the state of Chihuahua, Mexico. Annual accumulated radiation desert area (356.3 $kW \cdot m^{-2}$, 295–385 nm) was selected. In accordance with the Commission Internationale de l'Eclairage (CIE), the spectral range of (260–380 nm) of the Global Solar Spectral Irradiance represents only 4.2% of the annual solar radiation, as it represents the percentage of UV radiation at a wavelength equivalent to the Fluorescent UVA-340 lamp used on accelerated weathering chamber, with typical radiation of 0.77 $W \cdot m^{-2} \cdot nm^{-1}$. For general purposes, the energy contained in the 340 nm wavelength range is approximately 1% of this UV range. Knowing this, the annual UV radiation can be calculated using Equation (1), *i.e.*:

$$\text{Annual UV radiation } (kJ \cdot m^{-2}) = \text{Total solar radiation } (MJ \cdot m^{-2}) \times 1\% \times 1000 \text{ (kJ/MJ)} \quad (1)$$

So that:

$$\text{Annual UV radiation} = 3563 \text{ kJ} \cdot m^{-2} \quad (2)$$

Based on the parameters set and applied, the UV radiation emitted by the UVA-340 lamp is 0.77 $W \cdot m^{-2}$ at 340 nm.

According to the value obtained from radiant exposure (0.77 $W \cdot m^{-2}$) in the weathering chamber, the period to which the materials were subjected (56, 104, 176, 224, 272, 320 and 360 h) will accumulate the same annual UV radiation under normal weathering generated in ASTM D5272 test method and considering that radiant exposure is irradiance integrated over time. Therefore, the following equation applies:

$$(W \cdot m^{-2}) \times 3.6 \times \text{hours} = (kJ \cdot m^{-2}) \quad (3)$$

After performing a few algebraic functions:

$$(\text{light hours}) = \frac{\text{Annual UV radiation } (kJ \cdot W \cdot m^{-2})}{\text{radiant exposure } (W \cdot m^{-2}) \times 3.6} = \frac{3563 \text{ kJ} \cdot m^{-2}}{0.77 \text{ W} \cdot m^{-2}} \cong 1285 \text{ h} \quad (4)$$

With light hours per year, we calculate the Natural weathering, *i.e.*:

$$\text{Natural weathering (day)} = \frac{\text{Exposure time to UV (h)}}{\text{light hours}} \times 365 \text{ days} \quad (5)$$

Weathering conditions equivalences (natural and artificial) are shown in Table 4.

It was possible to simulate from 10 days of natural weathering during the shorter artificial exposure time (56 h) to 68 days of natural weathering during the longer artificial exposure time (360 h).

Table 4. Correlation of natural and artificial weathering.

Exposure time in artificial weathering (h)	Exposure time to UV (h)	Natural weathering (days)
56	37.33	10
104	69.33	19
176	117.33	33
224	149.33	42
272	181.33	51
320	213.33	60
360	240.00	68

5. Conclusions

Nanocomposites using amorphous and semicrystalline PLA were prepared by extrusion with 5 wt% load of an organomodified MMT type Cloisite30B. Through the processing conditions of extrusion and injection molding, they allowed us to obtain nanocomposites with a partially exfoliated structure within the PLA matrix. Clay galleries were broken down using applied shear forces during extrusion and injection. Particles that consist of well-aligned spaced platelets from 1.29 to 11.76 nm thickness were observed by TEM. A much larger decrease in nanocomposites' molecular weight compared to samples without C30B was observed. This effect can be attributed to the addition of C30B due to the strong interaction and miscibility between PLA and C30B, which originates from the strong hydrogen bonding among carboxyl groups of PLA and hydroxyl groups of C30B. The following conclusions can be derived from the aforementioned experimental results for the artificial weathering degradation for periods of up to 360 h. A major decrease in nanocomposites' molecular weight due to artificial weathering was also found, which can be attributed to the presence of C30B. Moreover, resistance to artificial weathering degradation was more pronounced in semicrystalline than amorphous PLA, independently of the presence of C30B. This may be due to the fact that the PLA chains arranged on crystalline regions degraded more slowly (k = 0.004 h^{-1}) than those in the amorphous regions (k = 0.0049–0.0052 h^{-1}). Even if a major decrease was observed in M_w compared to M_n on all tested materials the effect was more pronounced in nanocomposites test tubes than those without C30B. Submitting the test tubes under artificial weathering, it was possible to simulate from 10 days of natural weathering during the smaller artificial exposure time (56 h) to 68 days of natural weathering during the larger artificial exposure time (360 h). It was observed that no matter whether the PLA is semicrystalline or amorphous, the same exfoliation of the clay under the processing conditions was presented. Also, it was observed that the addition of clay favored PLA degradation in the amorphous regions, which means that semicrystalline regions in PLA-S were not affected during degradation in the presence of C30B.

Acknowledgments

The authors wish to thank the National Council for Science and Technology of México (CONACYT) for the grant awarded to Wendy Margarita Chávez-Montes. We wish to thank also to Carlos Elías Ornelas Gutiérrez, Víctor Manuel Orozco Carmona, Enrique Torres Moye, and

Daniel Lardizábal Gutiérrez for their valuable collaboration during this project. The authors acknowledge for technical support by the Nanotechnology National Laboratory at Centro de Investigación en Materiales Avanzados.

Author Contributions

Wendy Margarita Chávez-Montes, is the Ph. D. student whom performed all the packages and the overall experimental work. Guillermo González-Sánchez in CIMAV makes the TEM and XRD analysis, Ericka Ivonne López-Martínez perfomed the extrusion process optimization. Patricia de Lira-Gómez in Universidad Autónoma de Zacatecas, Lourdes Ballinas-Casarrubias in Universidad Autónoma de Chihuahua and Sergio Flores-Gallardo in CIMAV make artificial weathering analysis for molecular weight distribution.

Conflicts of Interest

The authors declare no conflict of interest.

References

1. Tsuji, H.; Echizen, Y.; Nishimura, Y. Photodegradation of biodegradable polyesters: A comprehensive study on poly(L-lactide) and poly(ε-caprolactone). *Polym. Degrad. Stab*. **2006**, *91*, 1128–1137.
2. Corti, A.; Solaro, R.; Chiellini, E. Biodegradation of poly(vinyl alcohol) in selected mixed microbial culture and relevant culture filtrate. *Polym. Degrad. Stab*. **2002**, *75*, 447–458.
3. Han, X.; Pan, J. Polymer chain scission, oligomer production. *Acta Biomater*. **2011**, *7*, 538–547.
4. Nieddu, E.; Mazzucco, L.; Gentile, P.; Benko, T.; Balbo, V.; Mandrile, R.; Ciardelli, G. Preparation and biodegradation of clay composites of PLA. *React. Funct. Polym*. **2009**, *69*, 371–379.
5. Lee, T.; Rasak, A.; Wan, A. *Polylactid Acid Handbook*, 1st ed.; Elsevier: New York, NY, USA, 2013.
6. Ho, C.; Wang, C.; Lin, C.; Lee, Y. Synthesis and characterization of TPO–PLA copolymer and its behavior as compatibilizer for PLA/TPO blends. *J. Polym.* **2008**, *49*, 3902–3910.
7. Conn, R.; Kolstad, J.; Borzelleca, J.; Dixler, D.; Filer, L., Jr.; LaDu, B.; Pariza, M. Safety assessment of polylactide (PLA) for use as a food-contact polymer. *Food Chem Toxic*. **1996**, *4*, 273–283.
8. Duncan, T. Applications of nanotechnology in food packaging and food safety: Barrier materials, antimicrobials and sensors. *J. Colloid Interface Sci*. **2011**, *363*, 1–24.
9. Mróz, P.; Białas, S.; Mucha, M.; Kaczmarek, H. Thermogravimetric and DSC testing of poly (lactic acid) nanocomposites. *Thermochim. Acta* **2013**, *573*, 186–192.
10. Luo, Z.; Koo, J. Quantification of the layer dispersion degree in polymer layered silicate nanocomposites by transmission electron microscopy. *J. Polym*. **2008**, *49*, 1841–1852.
11. Prasun, K.; Hakkarainen, M.; Albertsson, A. Nanoclay effects on the degradation process and product patterns of polylactide. *Polym. Degrad. Stab*. **2012**, *97*, 1254–1260.
12. Raquez, J.; Habibi, Y.; Murariu, M.; Dubois, P. Polylactide (PLA)-based nanocomposites. *Progress Polym. Sci*. **2013**, *38*, 1504–1542.

13. Najafi, N.; Heuzey, M.; Carreau, P. Polylactide (PLA)-clay nanocomposites prepared by melt compounding in the presence of a chain extender. *Compos. Sci. Technol*. **2011**, *72*, 608–615.
14. Lucas, N.; Bienaime, C.; Belloy, C.; Queneudec, M.; Silvestre, F.; Nava, J. Polymer biodegradation: Mechanisms and estimation techniques. *Chemosphere* **2008**, *73*, 429–442.
15. Zaidi, L.; Kaci, M.; Bruzaud, S.; Bourmaud, A.; Grohens, Y. Effect of natural weather on the structure and properties of polylactide/Cloisite 30B nanocomposites. *Polym. Degrad. Stab*. **2010**, *95*, 1751–1758.
16. Sotirios, I.; Zuburtikudis, I. Structure and thermal behavior of poly(L-lactic acid) clay nanocomposites: Effect of preparation method as a function of the nanofiller modification level. *J. Appl. Polym. Sci.* **2011**, doi:10.1002/app.35328.
17. Picard, E. Effect of an organo-modified montmorillonite on PLA crystallization and gas barrier properties. *Appl. Clay Sci.* **2011**, *53*, 58–65.
18. Paul, M.; Delcourt, C.; Alexandre, M.; Degee, P.; Monteverde, F.; Dubois, P. Polylactide/ montmorillonite nanocomposites: Study of the hydrolytic degradation. *Polym. Degrad. Stab.* **2005**, *87*, 535–542.
19. Perrin, F.; Ton, M.; Bureau, M.; Denault, J. Micro- and nano-structure in polypropylene/clay nanocomposites. *Polymer* **2005**, *46*, 11624–11634.
20. Mclauchlin, A.; Thomas, N. Preparation and thermal characterization of poly(lactic acid) nanocomposites prepared from organoclays based on an amphoteric surfactant. *Polym. Degrad. Stab.* **2009**, *94*, 868–872.
21. Lee, S.; Chen, H.; Milford, A. Preparation and characterization of tapioca starch–poly(lactic acid) nanocomposite foams by melt intercalation based on clay type. *Ind. Crops Product.* **2008**, *28*, 95–106.
22. Herrera, J.; Marand, E.; Little, J.; Cox, S. Polymer/clay nanocomposites as VOC barrier materials and coatings. *Polymer* **2009**, *50*, 5744–5748.
23. Degee, P.; Dubois, P.; Jerome, R. Bulk polymerization of lactides initiated by aluminium isopropoxide. *Macromol. Chem. Phys.* **1997**, *198*, 1985–1995.
24. Sakai, W.; Kinoshita, M.; Nagata, M.; Tsutsumi, N. ESR studies of photosensitized degradation of poly(L-lactic acid) via photoionization of dopant. *J. Polym. Sci. A Polym. Chem.* **2001**, *39*, 706–714.
25. Yasuda, N.; Wang, Y.; Tsukegi, T.; Shirai, T.; Nishida, H. Quantitative evaluation of photodegradation and racemization of poly(L-lactic acid) under UV-C irradiation. *Polym. Degrad. Stab.* **2010**, *95*, 1238–1243.
26. Santonja, L.; Ribes, A.; Alamo, R. Comparative thermal, biological and photodegradation kinetics of polylactide and effect on crystallization rates. *Polym. Degrad. Stab*. **2013**, *98*, 771–784.
27. Kumnayaka, T.; Parthasarathay, R.; Jollands, M.; Ivanov, I. Molecular weight changes during photo-oxidation of polyethylene nanocomposites. *Korea Aust. Rheol. J*. **2010**, *22*, 173–177.
28. Araujo, A.; Oliveira, M.; Oliveira, R.; Botelho, G.; Machado, A. Biodegradation assessment of PLA and its nanocomposites. *Environ. Sci. Pollut. Res*. **2014**, *21*, 9477–9486.